ISSN 2004-2965 Energy Proceedings, Vol. 20, 2021

**International Conference on Applied Energy 2021**
**Nov. 29 - Dec. 5, 2021, Thailand/Virtual**
**Paper ID: 616**

# A PARABOLIC PROTOTYPE OF SOLAR DRIVEN NATURAL GAS CHEMICAL LOOPING FOR SYNGAS PRODUCTION

Yali Cao[1,2], Xueli Xing[1,2], Hui Hong[1*]
[1] Institute of Engineering Thermophysics, Chinese Academy of Sciences, Beijing 100190, PR China
[2] University of Chinese Academy of Sciences, Beijing 100049, PR China

**ABSTRACT**

In this paper, a chemical looping fixed-bed reactor driven by concentrating solar energy was built, and the chemical looping cycle process of the solar syngas production was studied experimentally, which is the key reaction of the liquid sunshine production process. $N_2$ is used as a heat transfer medium to flow through the heat collecting tube and enter the reactor to provide heat for the reduction reaction. NiO is put into the reactor as an oxygen carrier, and methane is introduced as an oxygen carrier as fuel gas. The results show that with the development of the reaction process, the main reaction in the reactor has gradually changed from complete oxidation of methane to partial oxidation of methane. In this process, the methane conversion rate and the outlet syngas concentration are affected by the reaction temperature. Under the direct normal irradiation of over 860W/m$^2$, the methane conversion rate can reach up to 90%, and the outlet syngas concentration can be maintained at 50%. This paper also studied the chemical looping cycle reaction of methane under different irradiation intensities. The results show that when the DNI reaches 920W/m$^2$, the efficiency of solar energy to chemical energy can reach over 55%.

**Keywords:** Syngas production, Chemical looping process, Solar thermal energy, Parabolic trough concentrator

## NONMENCLATURE

| | |
|---|---|
| *Abbreviations* | |
| WS | Water Splitting |
| WGS | Water Gas Shift |
| CDS | Carbon Dioxide Splitting |
| YSZ | Yttria-Stabilized Zirconia |
| LHV | Low Heat Value |
| DNI | Direct Normal Irradiation |
| OC | Oxygen carrier |
| *Symbols* | |
| mi | Mass flow of Species i |
| $\theta$ | Incidence angle |
| $\theta_z$ | Zenith angle |
| $\beta$ | Rotation Tracking Angle |
| $\gamma_{solar}$ | Azimuth angle |
| $\gamma_{PTC}$ | Condenser azimuth |
| $\eta_{solar\text{-}to\text{-}chemical}$ | Solar energy to chemical energy efficiency |
| Cp | Specific heat |

## 1. INTRODUCTION

Solar energy is the most abundant source of energy on earth, providing about 885 TWh of energy per year[1]. But the solar energy is hard to use due to its decentralization and discontinuity[2]. If we want to capture, store and supply the sunlight as energy source, the key process is to convert it into a stable, storable, high energy-density chemical fuel.

The liquid sunshine is increasingly appealing to researchers[3]. Liquid sunlight is designed to convert sunlight into liquid fuels such as methanol. As the raw material of methanol production, the preparation of syngas via solar energy is a key process in current researches[4-7]. The conversion of solar to syngas is with the aid of chemical reactions. Such chemical reactions are natural gas steam reforming[8-10], coal gasification or biomass gasification[11, 12], or Water Splitting (WS) to hydrogen and oxygen. This last reaction can then be followed either by the Water Gas Shift (WGS) reaction or by the Carbon Dioxide Splitting (CDS) reaction to produce syngas[13, 14]. In these reactions, either the reaction temperature is high or $CO_2$ capture is needed. Therefore,

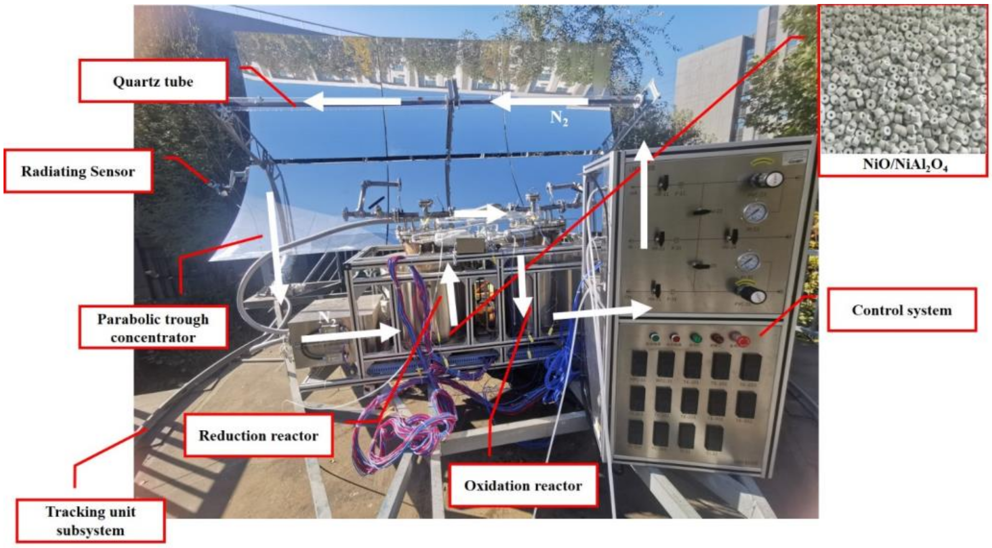


Fig.1 Concentrating solar energy driven double tank chemical looping fixed bed set up

it is urgent to develop a new syngas production method with the properties of low-temperature, clean, low carbon emission.

Chemical looping cycle was first proposed by Jin and Ishida in 1994[15]. Chemical looping process is a two-step redox cycle consisting of the partial oxidation of methane which is an endothermic reaction and the regeneration of oxygen carrier which is an exothermic reaction[16]. These two steps reactions are given by Eqs. (1) and (2), respectively[17].

$$\delta CH_4 + Me_xO_y \rightarrow \delta CO + 2\delta H_2 + Me_xO_{y-\delta} \quad (1)$$

$$Me_xO_{y-\delta} + \delta/2O_2 \rightarrow Me_xO_y \quad (2)$$

Solar thermal energy could be used as the heat source for the chemical looping syngas production. By means of the chemical looping process, the conversion of solar energy to chemical energy is completed.

The efficient development of chemical looping depends on favorable temperature matching and efficient oxygen carrier materials. Oxygen carrier is considered to be one of the most important factors. Among them, metal oxides are often used as oxygen carriers in the world [18-21]，NiO，$Fe_2O_3$，CuO and CoO have been studied by thermogravimetry or reactor. Jafarian et al.[22] discussed the influence of oxygen carrier type on the performance of solar chemical looping combustion system. We note that the performance of NiO is more competitive than other oxidation-reducing materials. Nickel-based oxides as redox materials have been studied and tested extensively in the literature. Ishida and Jin proposed a chemical looping combustion method using different carriers such as NiO and yttria-stabilized zirconia (YSZ)[23] and $NiAl_2O4$[24] as excellent media. In addition, the mixed metal oxide (CoO-NiO)/ YSZ[25], which is an excellent dielectric material, has been studied from the perspective of chemical kinetics and mechanical strength[26]. Therefore, NiO/$NiAl_2O_4$ is used as the oxygen carrier in this study.

## 2. EXPERIMENTAL SECTION

### *2.1 Experimental bench*

The syngas production performance is closely related to reaction kinetics and reaction selectivity, which are further determined by the distribution of oxygen carriers and the contact condition of the gas-solid reactants[27, 28]. In order to verify the experimental performance of syngas production by methane chemical looping driven by concentrating solar energy, we built a parabolic trough type syngas production principal prototype experimental platform via concentrating solar chemical looping, as shown in Figure 1. The experimental setup mainly includes the parabolic trough concentrator subsystem, the solar thermochemical hydrogen production subsystem, the tracking unit subsystem and other auxiliary equipment.

***Parabolic trough concentrator.*** The condenser surface has an ultrathin silver coating, by its use, the solar radiation reaching the mirror can be reflected to the collector tube with high reflectivity. The aperture width and length of the concentrator is 2550 mm and 4000mm, respectively. The outer diameter of the inner pipe of the collector tube is 38mm. The outer diameter of the covered glass tube is 102mm, and the vacuum structure between the outer glass tube and the inner tube is to reduce the heat dissipation penalty. The concentrated solar thermal energy from the mirror first reaches the inner tube surface through the covered glass tube and then converted into the thermal energy of $N_2$ by the coating through the inner tube surface. $N_2$ carries moderate-temperature heat as the driving force of the chemical looping reactions to achieve a conversion of solar energy to fuel chemical energy.

***Tracking unit subsystem.*** For the traditional trough single axis tracking method, the average annual optical efficiency is about 55%. The low optical efficiency is mainly caused by the large proportion of cosine loss. Taking winter as an example, cosine loss accounts for about 40% of the total incident energy[29]. Thus, it is the key to realize the efficient utilization of solar energy to reduce the cosine loss of concentrating process. According to Formula (3), reducing the incidence angle of sunlight is the breakthrough to reduce the cosine loss in the trough concentrating process. In this regard, Hong et al.[30] established the joint design of the azimuth of the sun and the condenser and proposed a new method for wide-angle tracking. By changing the concentrator azimuth $\gamma_{PTC}$ to further reduce the incidence angle $\theta$ of the sunlight, the relationship between the two is as follows:

$$\theta = \arccos\left[\cos\theta_z cos\beta + sin\beta sin\theta_z \cos(\gamma_{solar} - \gamma_{PTC})\right] \quad (3)$$

Based on the 300kWth rotatable-axis tracking solar parabolic-trough collector experimental platform, wide-angle tracking is applied to the prototype in this paper. A tracking method combining wide-angle tracking and axial movement is proposed, that is, horizontal rotation for solar azimuth tracking and axial rotation for solar zenith angle tracking. In this way, we can track the sun in both horizontal and axial directions in real time, and then the irradiation signal can be converted into digital signal via the program we write.

***Solar thermochemical looping fix-bed reactor.*** Based on the solar chemical looping process using methane and NiO to produce solar syngas, an experimental bench of fix-bed chemical looping reactor was designed and manufactured for studying the key reactions of the process. The schematic diagram of the chemical looping hydrogen production subsystem is shown in Fig.2. The experimental bench is made of two reactors, several mass flow controllers, an evaporator, several preheaters, and a gas analyzer. The chemical looping hydrogen production reactor was filled with 800g $NiO/NiAl_2O_4$ granular materials, in which the mass ratio of NiO to $NiAl_2O_4$ was 3:2. Natural gas is preheated and enters into the reduction reactor. NiO is employed as the oxygen carrier and reduced to Ni, and the gas products are CO, $CO_2$ and $H_2$, as shown in Eq (4) - (5). The reduction reaction is endothermic.

$$NiO + CH_4 \rightarrow Ni + CO + 2H_2 \quad (4)$$

$$4NiO + CH_4 \rightarrow 4Ni + CO_2 + 2H_2O \quad (5)$$

High-temperature nitrogen from the collector tube is piped into the reactor to provide heat for the endothermic reduction reaction. After heat exchange, $N_2$ still carries sensible heat, which can preheat the inlet methane feedstock. The N2 has residential heat, which can preheat the inlet NG. The product gas was collected by air bag and detected by Agilent gas chromatograph GC7890A. After the reduction reaction, the air releases $O^{2-}$ and oxidate Ni to NiO, as Eq (6) exhibited.

$$Ni + 0.5O_2 \rightarrow NiO \quad (6)$$

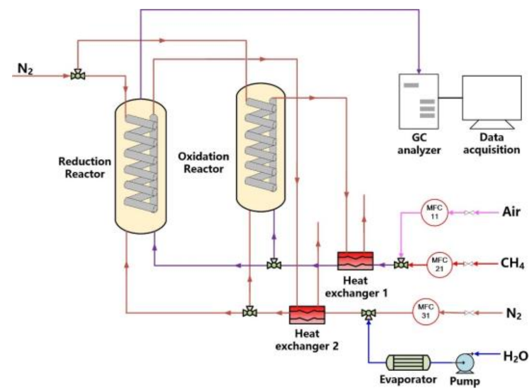


Fig.2 Schematic diagram of the experimental bench of double tank chemical looping reactor

## 2.2 Experimental materials

NiO is selected as the active component of oxygen carrier with $NiAl_2O_4$ doped into as the inert support material. The role of $NiAl_2O_4$ is to cover the active NiO phase and improve its resistance to sintering. The corresponding mass ratio of NiO to $NiAl_2O_4$ is 3:2. Based on this ratio, $Al(NO_3)_3 \cdot 9H_2O$ and $Ni(NO_3)_2 \cdot 6H_2O$ are weighed and dissolved in the mixture of isopropanol and deionized water. Stirring the solution for 1 h, then dry it at 80 °C for 12 h, at 150 °C for 24 h and at 200 °C for 5 h in a drying oven. NiO/ $NiAl_2O_4$ powders can be obtained after 3 h calcination in a muffle furnace at 500°C[31]. Last, the oxygen carrier product is obtained after pressing into shape in a tablet press.

## 2.3 Experimental evaluation

During the reduction reaction, methane is introduced into the fix-bed reactor at 500 ml/min. During the oxygen carrier regeneration stage, air is fed at 900°C. The processes are all controlled by an integrated controller and operated at one atmospheric pressure. The experimental data is analyzed based on the composition of gas at the reactor outlet, which is collected and detected by gas chromatography.

Solar to chemical energy efficiency and syngas selectivity were selected to evaluate the thermodynamic performance of concentrating solar methane chemical looping reaction,

$$\eta_{solar-to-chemical} = \frac{\dot{m}_{H2}LHV_{H2}+\dot{m}_{CO}LHV_{CO}+Q_{Ni}-\dot{m}_{CH4}LHV_{CH4}}{DNI\times S}\times 100\% \qquad (7)$$

$$syngas\ selectivity = \frac{n_{CO}+n_{H2}}{n_{CO}+n_{H2}+n_{CO2}}\times 100\% \qquad (8)$$

where $DNI$ represents the direct normal irradiation and $S$ represents the mirror field area. $m_{H2}$、$m_{CO}$ and $m_{CH4}$ represent the flow rate of $H_2$, CO and $CH_4$ respectively. $LHV$ represents the low heat value of the fuel. $X_{CH4}$ is the conversion rate of methane.

## 3. RESULT AND DISCUSSION

The experimental study on the concentrated solar chemical looping fixed bed reactor using methane and NiO/ $NiAl_2O_4$ was carried out. Under the conditions of nitrogen flow rate of 550L/min and heat collector efficiency of 0.68, we measured the nitrogen temperature at the outlet of the collector tube under different irradiation intensities on different days, and they basically fell on a straight line, shown as Fig.3.

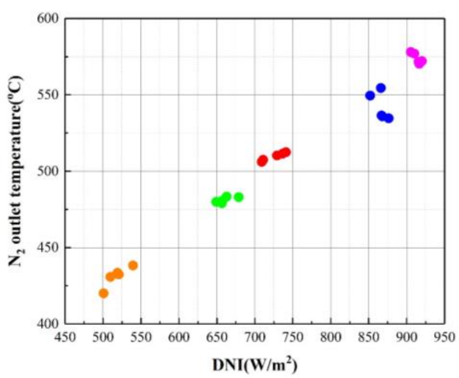


Fig.3 $N_2$ outlet temperature of the collector tube under different DNI

We investigated the results of methane chemical looping experiments under different DNI. The reduction behavior of 800g NiO/ $NiAl_2O_4$ under a stream of 500 ml/min methane is presented in Fig.4 to 6. The concentrations of outlet gas were detected by the chromatography, and the results of the first 2400s were selected as the basis for studying. The results show that methane conversion increases with the increase of DNI and reaction temperature. We analyzed the experimental results under different DNI, as shown in Figure 4. Under low irradiation (Fig.4 (a)), the reaction rate of methane is low, and the conversion begins after 900s. However, under high irradiation (Fig.4 (b) and (c)), the methane conversion rate increase with the increase of irradiation intensity. In the initial stage of the reaction (before 1200s-1500s), the concentration of $CO_2$ is higher than syngas concentration, and the syngas concentration gradually increases in the later stage of the reaction. This might be due to the high reaction temperature is more conducive to the release of oxygen of OCs at the initial stage of the reaction, which makes it easier for methane to be completely oxidized into $CO_2$ rather than CO. The main reaction occurring at this time is as follows:

$$NiO + 1/4\ \delta CH_4 \rightarrow NiO_{1-\delta} + 1/4\ \delta CO_2 + 1/2\ \delta H_2O \qquad (9)$$

With the progress of the reaction, the concentration of syngas increases gradually, and the syngas content exceeds that of $CO_2$ in about 1300s. Afterwards, the concentration of syngas continues to rise while the concentration of $CO_2$ continues to fall. As for Fig.4 (b) and (c), the reaction goes to 1700s, the concentration of syngas is above 50% and trends to be stable, and the concentration of $CO_2$ would be less than 30%. The reason might be that, as the reaction conducted, increased diffusion resistance results in inadequate contact between methane and oxygen carriers, and the decrease of oxygen transfer rate. Less oxygen is transferred to react with methane. More methane is partially oxidized to form CO and hydrogen rather $CO_2$.

Figure 5 shows the change of methane conversion rate within the irradiation time of 2400s. It can be seen that when the DNI reach 860W/m$^2$ and 920 W/m$^2$, the methane conversion rate reaches the highest at about

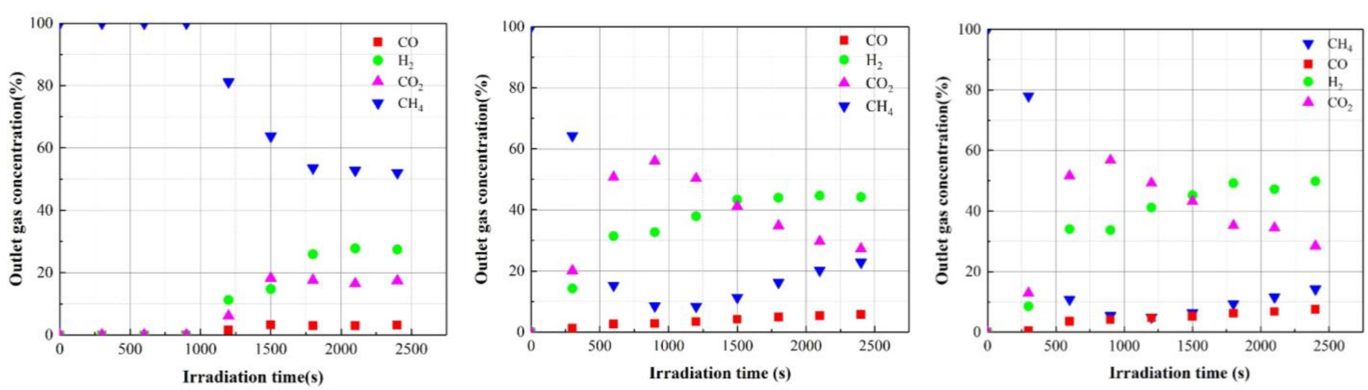


Fig.4 Composition of outlet gas at different DNI ($FCH_4$=0.5L/min,10% vol)

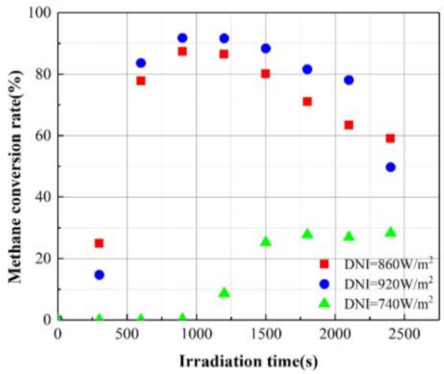


Fig.5 $CH_4$ conversion rate under different DNI

1000s, which is 87.35% and 91.74%, respectively. Accordingly, the syngas selectivity is 64.65% and 66.83%, respectively.

Figure 6 shows the solar-to-chemical efficiency under different DNI. According to Equation (7), the solar to chemical energy efficiency is a function of the methane conversion rate $X_{CH4}$ and the direct irradiation intensity DNI. The dots represent the solar-to-chemical efficiency of experiments conducted on different dates and DNI. As can be seen from the figure, the conversion efficiency of solar energy to chemical energy increases with the increase of the irradiation intensity from 700W/$m^2$ to 950W/$^2$. That might be that, the increase of irradiation intensity makes the nitrogen outlet temperature higher and carries more heat to supply the reduction reaction. With the progress of the reaction, the methane conversion gradually increased, the synthesis gas also gradually increased. When the irradiation intensity exceeds 900W/$m^2$, the efficiency of solar-to-chemical can exceed 40%. According to the experimental results, the fitting curve of solar energy to chemical energy efficiency was obtained, which is the sigmoid function.

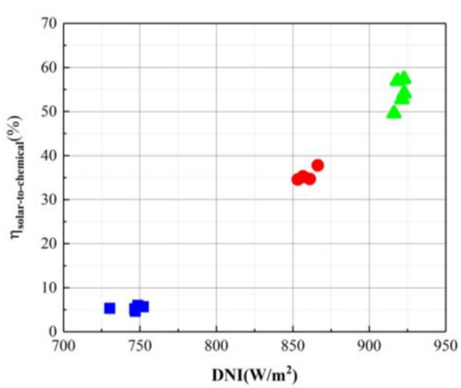


Fig. 6 Solar-to-chemical efficiency under different DNI

## CONCLUSIONS

In this study, the chemical looping process using methane for syngas production driven by concentrating solar is experimentally analyzed. $NiO/NiAl_2O_4$ is selected as the oxygen carrier and the reaction is conducted under different DNI. With the development of chemical looping process, the major reaction changes from the complete oxidation of methane to the partial oxidation of methane. This means that in order to obtain syngas as the product, the reaction temperature needs to be maintained within the optimal range. At the DNI of 860W/$m^2$, the temperature in the reduction reactor is about 450$^o$C. The methane conversion can reach 87.35% and the syngas selectivity is 64.65%. We studied the reaction of $CH_4$ to syngas via chemical looping cycle under different direct irradiation intensities. Methane conversion increases with the increase of DNI, and when DNI exceeds 900W/$m^2$, methane conversion can reach 90%, with the solar energy to chemical energy efficiency of over 55%.

## ACKNOWLEDGEMENT

The authors gratefully acknowledge the support of the Basic Science Center Program for Ordered Energy Conversion of the National Natural Science Foundation of China (No. 51888103), National Natural Science Foundation of China (No. 51906245), and the Beijing Key Laboratory of Distributed Combined Cooling Heating and Power System.

## REFERENCE

1. *Solar Energy Perspectives*; International Energy Agency 2011.
2. Srirat, C.; Stéphane, A.; Sylvain, R., Syngas production via solar-driven chemical looping methane reforming from redox cycling of ceria porous foam in a volumetric solar reactor. *Chemical Engineering Journal* **2018,** *356*, 756-770.
3. Shih, C. F.; Tao, Z.; Li, J.; Bai, C., Powering the Future with Liquid Sunshine. *Joule* **2018,** *2* (10).
4. Steinfeld, A., Solar thermochemical production of hydrogen—a review. *Solar Energy* **2006,** *78* (5), 603-615.
5. Navarro, R. M.; Pena, M. A.; Fierro, J., Hydrogen Production Reactions from Carbon Feedstocks: Fossil Fuels and Biomass. *Cheminform* **2007,** *38* (50), 3952-3991.
6. Turner, J. A., Sustainable hydrogen production. *Science* **2004,** *305* (5686), 4.
7. Svoboda, K.; Slowinski, G.; J.Rogut, Thermodynamic possibilities and constraints for pure hydrogen production by a nickel and cobalt-based

 

chemical looping process at lower temperatures. *Energy Conversion Management* **2007**.

8. Anik Ee V, V. I.; Bobrin, A. S.; Ortner, J.; Schmidt, S.; Funken, K. H.; Kuzin, N. A., Catalytic thermochemical reactor/receiver for solar reforming of natural gas: Design and performance. *Solar Energy* **1998,** *63* (2), 97-104.
9. Hirsch, D.; Epstein, M.; Steinfeld, A., The solar thermal decarbonization of natural gas. *International Journal of Hydrogen Energy* **2001,** *26* (10), 1023-1033.
10. Möller, S.; Kaucic, D.; Sattler, C., Hydrogen Production by Solar Reforming of Natural Gas: A Comparison Study of Two Possible Process Configurations. *Journal of Solar Energy Engineering* **2005,** *128* (1), 16-23.
11. Flechsenhar, M.; Sasse, C., Solar gasification of biomass using oil shale and coal as candidate materials. *Energy* **1995,** *20* (8), 803-810.
12. Trommer, D.; Noembrini, F.; Fasciana, M.; Rodriguez, D.; Morales, A.; Romero, M.; Steinfeld, A., Hydrogen production by steam-gasification of petroleum coke using concentrated solar power—I. Thermodynamic and kinetic analyses. *International Journal of Hydrogen Energy* **2007,** *30* (6), 605-618.
13. Miller, J., Initial case for splitting carbon dioxide to carbon monoxide and oxygen. *sandia report sand* **2007**.
14. Chueh, W.; Haile, S., Ceria as a Thermochemical Reaction Medium for Selectively Generating Syngas or Methane from H2O and CO2. *ChemSusChem* **2010,** *2*.
15. Ishida, M.; Jin, H., A new advanced power-generation system using chemical-looping combustion. *Energy* **1994,** *19* (4), 415-422.
16. Jiang, Q.; Zhang, H.; Cao, Y.; Hong, H.; Jin, H., Solar hydrogen production via perovskite-based chemical-looping steam methane reforming. *Energy Conversion and Management* **2019,** *187* (MAY), 523-536.
17. Akbari-Emadabadi, S.; Rahimpour, M. R.; Hafizi, A.; Keshavarz, P., Production of hydrogen-rich syngas using Zr modified Ca-Co bifunctional catalyst-sorbent in chemical looping steam methane reforming. *Applied Energy* **2017,** *206*, 51-62.
18. Qiongqiong Jiang, H. Z., Yali Cao, Hui Hong∗, Hongguang Jin, Solar hydrogen production via perovskite-based chemical-looping steam methane reforming. *Energy Conversion and Management* **2019,** (187), 523-536.
19. Mattisson, T.; Johansson, M.; Lyngfelt, A., The use of NiO as an oxygen carrier in chemical-looping combustion. *Fuel* **2006,** *85* (5-6), 736-747.
20. In *Reactivity Study of Co-based Oxygen Carrier for Chemical-looping Combustion*, Proceedings of the 8th International Conference on Measurement and Control of Granular Materials, 2009.
21. He, F.; Wang, H.; Dai, Y., Application of Fe2O3/Al2O3 Composite Particles as Oxygen Carrier of Chemical Looping Combustion. *Journal of Natural Gas Chemistry* **2007,** *16* (2), 155-161.
22. Cho, P.; Mattisson, T.; Lyngfelt, A., Comparison of iron-, nickel-, copper- and manganese-based oxygen carriers for chemical-looping combustion. *Fuel* **2004,** *83* (9), 1215-1225.
23. Liu, K.; Song, C.; Subramani, V., Hydrogen and Syngas Production and Purification Technologies (Liu/Hydrogen and Syngas) || Color Plates. **2009**, c1-c12.
24. Zhaosong Sun; Hao Liang; Yin., Z., Research development in chemical looping process for hydrogen generation. *Chemical Industry and Engineering* **2015,** *32* (05), 71-78.
25. Jin, H.; Ishida, M., Reactivity Study on Natural-Gas-Fueled Chemical-Looping Combustion by a Fixed-Bed Reactor. *Industrial Engineering Chemistry Research* **2002,** *41* (16), 4004-4007.
26. Jin, H.; Okamoto, T.; Ishida, M., Development of a Novel Chemical-Looping Combustion: Synthesis of a Looping Material with a Double Metal Oxide of CoONiO. *Energy&Fuels* **1998,** *12* (6), 1272-1277.
27. Zhang, H.; Liu, X.; Hong, H.; Jin, H., Characteristics of a 10 kW honeycomb reactor for natural gas fueled chemical-looping combustion. *Applied Energy* **2018,** *213* (mar.1), 285-292.
28. Liu, X.; Zhang, H.; Hong, H.; Jin, H., Experimental study on honeycomb reactor using methane via chemical looping cycle for solar syngas. *Applied Energy* **2020,** *268*, 114995.
29. Wang, R. The evaluation of solar-aided coal-fired power generation system and the active-regulation mechanism of the solar concentrating and conversion. University of Chinese Academy of Sciences.
30. Peng; Hong; Jin; HG; Zhang; ZN, A new rotatable-axis tracking solar parabolic-trough collector for solar-hybrid coal-fired power plants. *solar energy* **2013**.
31. Zhang, H.; Hong, H.; Jiang, Q.; Deng, Y.; Jin, H.; Kang, Q., Development of a chemical-looping combustion reactor having porous honeycomb chamber and experimental validation by using NiO/NiAl2O4. *APPLIED ENERGY* **2018,** *211* (FEB.1), 259-268.

 